

# Polarized Multi-Channel Transmit MRI to Reduce B1-Shading near Metal Implants

Theresa Bachschmidt<sup>1,2</sup>, Peter Jakob<sup>2</sup>, Markus Vester<sup>1</sup>, Jürgen Nistler<sup>1</sup>, and Mathias Nittka<sup>1</sup>

<sup>1</sup>Siemens Healthcare, Erlangen, Germany, <sup>2</sup>Experimental Physics 5, University of Würzburg, Würzburg, Germany

## Introduction

The main source of metal artifacts is susceptibility-induced distortion, which is addressed by various methods (SEMAC [1], MAVRIC [2]). Hence, other types of artifacts become more prominent: shading and banding in the vicinity of the femoral part of a total hip arthroplasty (THA) implant at 3T [3,4], caused by induced RF currents superimposing with the external  $B_1$  field. These effects are not relevant at 1.5T. This work aims to systematically analyze  $B_1$  modulations and investigate a new approach to reduce those by means of  $B_1$  polarization, using state-of-the-art multi-channel transmit (TX) MRI systems. Simulations, phantom measurements and first clinical results are presented.

## Methods

An infinitely long cylinder filled with water and a metal rod of defined length  $l_R$  and diameter inserted in the cylinder in parallel to the body coil at different positions  $\mathbf{p} = (x_p, y_p)$ , assuming lossless interaction with the surrounding medium and no susceptibility effects, form the model. The central transverse section is observed. A pair of linearly polarized exciting fields  $B_1^x$  and  $B_1^y$  applied along the x- and y-axes give rise to vector potentials  $\mathbf{A}^x$  and  $\mathbf{A}^y$  along the z-axis inside the cylinder [5]. The combined vector potential  $\mathbf{A}^t = \text{real}(\mathbf{A} \cdot e^{i\omega t})$  with  $\mathbf{A} = \mathbf{A}^x e^{i\varphi} + \mathbf{A}^y$  contains all information about phase and amplitude (circular polarization (CP):  $B_1^x = B_1^y$ ,  $\varphi = 90^\circ$ ) and results in the magnetic field  $\mathbf{B} = \text{curl} \mathbf{A}^t$ . The associated electric field inside the cylinder is given by  $\mathbf{E}(\mathbf{r}) = i\omega/2 \mathbf{r} \times \mathbf{B}(\mathbf{r})$  and gives rise to an electric current  $I_z \approx E_z(\mathbf{p})l_R/(i\omega L_R)$  in the rod with an inductance  $L_R$ . The induced magnetic field inside the bottle at each position (cf. figure 1) can be calculated according to

$$B_x^{\text{ind}}(\mathbf{r}) = -\frac{\mu_0}{2\pi} \frac{\sin(\psi_r)}{r_p} I_z, \quad B_y^{\text{ind}}(\mathbf{r}) = \frac{\mu_0}{2\pi} \frac{\cos(\psi_r)}{r_p} I_z$$

Infinite propagation speed is assumed in the model. The resulting induced and undistorted MR-effective fields  $B_{\text{MR}}^{\text{ind}}$  and  $B_{\text{MR}}^{\text{orig}}$ , which superimpose and form the total transmit field  $B_{\text{MR}}^{\text{tot}}$ , are

$$B_{\text{MR}}^{\text{ind}}(\mathbf{r}) \propto \frac{\sin(\psi_r) + i \cos(\psi_r)}{r_p} (y_p \partial_y + x_p \partial_x) \mathbf{A}(\mathbf{p}), \quad B_{\text{MR}}^{\text{orig}}(\mathbf{r}) = (\partial_y + i \partial_x) \mathbf{A}(\mathbf{r})$$

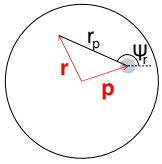


Fig.1: Parameters

$B_{\text{MR}}^{\text{tot}}$  depends not only on the polarization of the transmit field, but also on the position of the rod. The analytical model is validated by numerical finite-element simulation (CST Studio). Analytical calculations are performed for circularly and elliptically polarized ( $EP_1$ :  $B_1^x=0.98$ ,  $B_1^y=0.2$ ,  $\varphi=110^\circ$ ) transmit fields and verified experimentally for the following setup: a titanium rod (length 0.2m,  $\varnothing 1.2\text{cm}$ ) is placed off-center at  $\mathbf{p} = (5\text{cm}, 0)$  in a cylinder with doped water (length 36cm,  $\varnothing 17\text{cm}$ ,  $\sigma=0.83\text{S/m}$ ) in a 3T MR system. The body coil is used for both transmission and reception and  $B_1$  mapping is performed, using the method introduced in [6]. In vivo, a THA patient is measured in two differently polarized modes (CP and  $EP_2$ :  $B_1^x=0.88$ ,  $B_1^y=0.48$ ,  $\varphi=130^\circ$ ) with a turbo spin echo sequence (TSE) in coronal plane. This is compared to the theoretical  $B_1$  distribution and the spin echo (SE) signal intensity obtained by  $\sin^3(\pi/2 \cdot c)$ , while  $c \propto B_1$ .

The underlying model is a cylindrical geometry approximating the shape of the body (cylinder:  $\varnothing 0.32\text{m}$ ; rod:  $\varnothing 2\text{cm}$ , length 0.14m, 0.1m off-center).

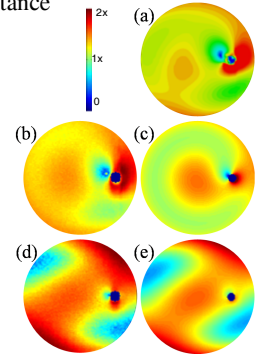


Fig.2: Numerical (a) and analytical (c,e) simulations and measurements (b,d)

## Results

Figure 2 shows the results for phantom experiments and simulations. For the  $B_1$  field in the CP mode (a-c), numerical (a) and analytical (c) simulations and experiment (b) are in good agreement in proximity to the metal. The perturbation in this area is significant, especially the increase on its right. Although elliptical excitation ( $EP_1$ ) degrades the overall field homogeneity (experiment (d), simulation (e)), the  $B_1$  field close to the metal is more homogeneous compared to the CP mode and features lower gradients. Using this polarization for a rod rotated by  $30^\circ$  about z, inhomogeneities comparable to the CP mode (b,c) occur (without figure). The intensity pattern can be predicted by the simplified model, but the rod causes stronger  $B_1$  effects in the experiment. In-vivo results acquired in CP mode (fig. 3a) show shading on the right side of the implant, which does not occur in the  $EP_2$  mode (b). Corresponding simulations show the same signal intensity patterns in the SE images (c,d). The red lines indicate the signal modulation for a central coronal slice. Regarding the  $B_1$  distribution, a significant increase in  $B_1$  in the CP mode in the area of shading is visible compared to a moderate increase in the  $EP_2$  mode in the respective area (blue lines in (c,d)).

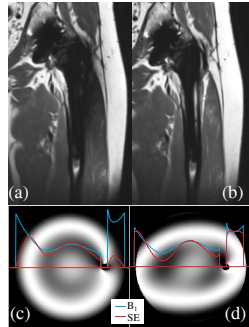


Fig.3: In vivo results and simulation in CP (a,c) and  $EP_2$  mode (b,d)

## Discussion

Significant changes of the  $B_1$  field close to the implant are translated to changes in image brightness and contrast, depending on the applied imaging technique. In particular, sharp transitions between hypo- and hyper-intense signals may occur, mimicking anatomical structures and thus increase the risk of misinterpretations. Theoretical and experimental results demonstrate that the intensity and spatial pattern of this effect does not only depend on the geometrical and electrical properties of the object to be imaged, but also on the polarization of the TX field. In this study, an electrodynamic field analysis of a simplified model allowed to predict the observed effects in good agreement with numerical simulations and experiments. However, only RF fields were considered; other effects such as eddy currents induced by low-frequency imaging gradients [7] were neglected.

## Conclusion

While multi-channel TX systems are usually focused on  $B_1$  homogenization or accelerated 2D-selective RF pulses, here a new application to reduce metal artifacts is presented. Based on our findings, the polarization of the TX field may be optimized to reduce the impact of induced  $B_1$  fields near metal implants. However, we recognize that some areas in the image may be improved, whereas others may be degraded.

**References** [1] Lu et al MRM, 2009; 62(1):66-76, [2] Koch et al 2009 MRM 61:381-390, [3] Koch et al ISMRM 2010; p 3082, [4] Graf et al, MRI, 23, 2005, 493-499, [5] Tropp JMR, 2004; 167:12-24, [6] Fautz et al ISMRM 2008, 1247, [7] Graf et al MRM, 2005, 54:231-234